Cardiovascular Research (2010) **85**, 464–472
doi:10.1093/cvr/cvp336

Influence of heart failure on nucleocytoplasmic transport in human cardiomyocytes

Raquel Cortés[1†], Esther Roselló-Lletí[1†], Miguel Rivera[1], Luis Martínez-Dolz[2], Antonio Salvador[2], Inmaculada Azorín[3], and Manuel Portolés[4*]

[1]Cardiocirculatory Unit, Research Center, Hospital Universitario La Fe, Valencia, Spain; [2]Cardiology Unit, Hospital Universitario La Fe, Valencia, Spain; [3]Experimental Neurology, Research Center, Hospital Universitario La Fe, Valencia, Spain; and [4]Cell Biology and Pathology Unit, Research Center, Hospital Universitario La Fe, Avd. Campanar, 21, Valencia 46009, Spain

Received 17 July 2009; revised 17 September 2009; accepted 6 October 2009; online publish-ahead-of-print 9 October 2009

Time for primary review: 23 days

Aims The role of the cell nucleus in the development of heart failure (HF) is unknown, so the objectives of this study were to analyse the effect of HF on nucleocytoplasmic transport and density of the nuclear pore complex (NPC).

Methods and results A total of 51 human heart samples from ischaemic (ICM, $n = 30$) and dilated (DCM, $n = 16$) patients undergoing heart transplantation and control donors (CNT, $n = 5$) were analysed by western blotting. Subcellular distribution of proteins and NPC were analysed by fluorescence and electron microscopy, respectively. When we compared nucleocytoplasmic machinery protein levels according to aetiology of HF, ICM showed higher levels of importins [(IMP-β3) (150%, $P < 0.0001$), IMP-α2 (69%, $P = 0.001$)] and exportins [EXP-1 (178%, $P < 0.0001$), EXP-4 (81%, $P = 0.006$)] than those of the CNT group. Furthermore, DCM also showed significant differences for IMP-β3 (192%, $P < 0.0001$), IMP-α2 (52%, $P = 0.025$), and EXP-1 (228%, $P < 0.0001$). RanGTPase-activating proteins (RanGAP1 and RaGAP1^{u}) were increased in ICM (76%, $P = 0.005$; 51%, $P = 0.012$) and DCM (41%, $P = 0.042$; 50%, $P = 0.029$). Furthermore, subcellular distribution of nucleocytoplasmic machinery was not altered in pathological hearts. Finally, nucleoporin (Nup) p62 was increased in ICM (80%) and DCM (109%) ($P < 0.001$ and $P = 0.024$). Nuclear pore density was comparable in pathological and CNT hearts, and ICM showed a low diameter ($P = 0.005$) and different structural configuration of NPC.

Conclusion This study shows the effect of HF on nucleocytoplasmic trafficking machinery, evidenced by higher levels of importins, exportins, Ran regulators and Nup p62 in ischaemic and dilated human hearts than those in the controls, with NPCs acquiring a different configuration and morphology in ICM.

Keywords Heart failure • Ischaemia • Human cardiomyocytes • Nucleocytoplasmic transport

1. Introduction

Heart failure (HF) has been associated with changes in glycolytic enzymes, mitochondria, and cytoskeletal proteins.[1–4] However, molecular mechanisms, such as changes in the expression of genes and proteins of myocardium, have not been well established, especially in the role of the nucleus in the development of HF despite the importance of this structure in the cellular biology.

In the nucleus of eukaryotic cells several processes essential for cell life, such as gene expression, signal transduction, and cell cycle progression occur.[5] These processes require a precise regulation through a selective bidirectional transport between the nucleus and the cytoplasm of most proteins, including membrane proteins, enzymes, ribosomal subunits, and some types of RNAs. The transport of macromolecules across the nuclear envelope is mediated by the nuclear pore complex (NPC). Several authors have demonstrated that the nuclear transport infrastructure can be altered and adopt distinct conformations, determining the traffic of macromolecules across the nuclear pore, in cardiomyocyte culture and cardiomyocytes infected with different cardioviruses.[6–8]

†The first two authors contributed equally to the study.

* Corresponding author. Tel: +34 96 386 27 00, Fax: +34 96 197 30 18, Email: portoles_man@gva.es

Import/export of these cargo proteins requires the participation of transport factors referred to as importins (IMPs) and exportins (EXPs).[9] The IMPs bind to the nuclear localization signal (NLS) in the cargoes and move them to the nucleus and EXPs bind to the nuclear export signal (NES) in the cargoes and ensure its transport to the cytoplasm.[10] Passage through the NPC is mediated by transient IMPs/NLS-protein complex with FG-nucleoporin (Nup) interactions, such as Nup p62.[11] The release within the nucleus at the end of the IMP process requires the interaction of the IMPs/NLS-protein complex with Ran in activated GTP-bound form (RanGTP) to dissociate the transport complex.[12] Nuclear protein export is analogous to nuclear import, with the exception that EXPs are involved. Dependent on RanGTP, EXPs recognize NES,[13] the complex of EXP/NES-protein/RanGTP moving through the NPC via Nup interactions, and the complex is dissociated in the cytoplasm by RanGAP (RanGTPase-activating protein), which catalyzes GTP hydrolysis together with the coactivator Ran binding protein, RanBP1.[14] Thus, the NPC, in association with several carriers and their regulators, is responsible for the recognition and translocation of specific cargoes in and out of the nucleus, thereby controlling the distribution of the proteins.

The objectives of this study were to analyse the influence of HF on several aspects of the nucleus in human cardiomyocytes through the analysis of the potential alterations in the nucleocytoplasmic transport and in the density of NPC by electron microscopy. Therefore, we have analysed different representative transport factors: IMP-β3 (which imports histones and ribosomal proteins), the most studied adapter protein IMP-α2, EXP-1 (involves in the nuclear export of several shuttling proteins), and EXP-4 (which exports eIF5A). In addition, we also determined the amount of Ran-related factors (RanGAP1, RanGAP1^u, and RanBP1) and Nup p62.

2. Methods

2.1 Source of tissue

A total of 46 explanted human hearts were obtained from 30 patients with ischaemic cardiomyopathy (ICM) and 16 with dilated cardiomyopathy (DCM) undergoing cardiac transplantation. Clinical history, ECG, echocardiography, haemodynamic studies, and coronary angiography data were available on all patients. Non-ischaemic DCM was diagnosed when patients had intact coronary arteries on coronary angiography and LV systolic dysfunction (EF $<$ 40%) with a dilated non-hypertrophic LV (LVDD $>$ 55 mm) on echocardiography. Furthermore, patients did not show existence of primary valvular disease. All patients were functionally classified according to the New York Heart Association (NYHA) criteria and were receiving medical treatment following the guidelines of the European Society of Cardiology.[15]

Five non-diseased donor hearts were used as control (CNT) samples. The hearts were initially considered for cardiac transplantation but were subsequently deemed unsuitable for transplantation either because of blood type or size incompatibility. The cause of death was cerebrovascular accident or motor vehicle accident. All donors had normal LV function and no history of myocardial disease or active infection at the time of transplantation.

Transmural samples were taken from near the apex of the left ventricle. The DCM, ICM, and CNT samples were flushed with 0.9% NaCl and stored at 4°C for a mean time of 4.18 $\pm$ 3.07 h from loss of coronary circulation. All tissues were obtained with informed consent of patients. The project was approved by the Ethics Committee of our hospital and conducted in accordance with the guidelines of the Declaration of Helsinki.

2.2 Homogenization of samples and protein determination

Hundred milligram of frozen left ventricle was transferred into Lysing Matrix tubes designed for use with the FastPrep-24 homogenizer (MP Biomedicals, USA) in a total protein extraction buffer (2% SDS, 250 mM sucrose, 75 mM urea, 1 mM dithiothreitol, and 50 mM Tris–HCl, pH 7.5) with protease inhibitor (25 μg/mL aprotinin and 10 μg/mL leupeptin). The homogenates were centrifuged and supernatant aliquoted. The protein content of the aliquot was determined by the Lowry method[16] using bovine serum albumin (BSA) as standard.

2.3 Polyacrylamide gel electrophoresis and western blot analysis

Samples were separated by Bis-Tris Midi gel electrophoresis with 4–12% polyacrylamide in a separate gel for IMP-β3, IMP-α2, EXP-1, EXP-4, RanGAP1, RanGAP1^u, RanBP1, and Nup p62. After electrophoresis, the proteins were transferred from the gel to a PVDF membrane by the iBlot Dry Blotting System (Invitrogen Ltd, UK) for western blot. After blocking all night in the refrigerator with 1% BSA in Tris-buffer solution containing 0.05% Tween 20, membranes were incubated for 2 h with a primary antibody in the same buffer. The primary detection antibodies used were: anti-IMP-α2 rabbit polyclonal antibody, anti-IMP-β3 monoclonal antibody, anti-EXP-4 goat polyclonal antibody, anti-p62 rabbit polyclonal antibody, anti-RanGAP1 and RanGAP1^u monoclonal antibody, and anti-RanBP1 rabbit polyclonal antibody, from Santa Cruz Biotechnology, Inc. (Heidelberg, Germany). Anti-EXP-1 monoclonal antibody was from BD Biosciences (San Jose, CA, USA). Monoclonal anti-β-actin antibody (Sigma-Aldrich, Missouri, USA) was used as loading CNT of each of the blots.

Then, the bands were visualized using an acid phosphatase-conjugated secondary antibody and nitro blue tetrazolium/5-bromo-4-chloro-3-indolyl phosphate (Sigma) substrate system. Finally, bands were digitalized using an image analyser (DNR Bio-Imaging Systems) and quantified by the Gel Capture (v.4.30) and the TotalLab TL-100 (v.2008) programs.

2.4 Fluorescence microscopy

To analyse protein distribution, frozen muscular sections were transferred to glass slides, fixed in 4% paraformaldehyde for 15 min at 4°C. Then samples were blocked with PBS containing 1% BSA for 15 min at room temperature. After blocking, sections were incubated for 90 min at 37°C with the primary antibodies (described in western blot analysis) in the same buffer solution, and then with FITC-conjugated secondary antibody (Santa Cruz Biotechnology INC) for 60 min at room temperature.[17] Finally, sections were rinsed in PBS, mounted in Vectashield (Vector), and observed with an Olympus B$\times$50 fluorescence microscope. The images were processed with ImageJ (v. 1.4.3.67) program.

2.5 Tissue processing for electron microscopy

Myocardial samples (size 1 mm^3) from left ventricle were fixed in a solution of 1.5% glutaraldehyde plus 1% formaldehyde in 0.05 M cacodylate buffer, pH 7.4, for 60 min at 4°C. Then, samples were post-fixed in 1% OsO_4 for 60 min at 4°C, dehydrated in ethanol and embedded in Epon 812. Two types of sectioning were obtained, 1.5 μm semi-thin sections stained with toulidine 0.5%, for observation with light microscopy; and 60 nm ultra-thin sections mounted on nickel grids

and counter-stained with 2% uranyl acetate for 20 min and 2.7% lead citrate for 3 min,[18] for electron microscopy observation, using a Philips CM-100, with magnifications ranging for ×4500–15000.

A quantitative stereological analysis of the photomicrographs was performed to quantify the numerical density and distribution of NPC by iTEM FEI program (v. 5.0, 2008) by Olympus Soft Imaging Solutions GmbH, with the scientifical criteria described by Marín *et al.*[19]

2.6 Statistical methods

Data are presented as the mean value ± standard deviation. The Kolmogorov–Smirnov test was used to analyse the distribution of the variables. Comparisons of clinical characteristics were achieved using Student's *t*-test for continuous variables and Fisher exact test for discrete variables. Comparisons of nuclear protein levels and nuclear pores distribution between two groups were performed using the Mann–Whitney *U* test, and comparisons between three groups were performed with a Kruskal–Wallis test. Significance was assumed as $P < 0.05$. All statistical analyses were performed using SPSS software v. 11.5 for Windows (SPSS Inc.).

3. Results

3.1 Clinical characteristics of patients

Most of the patients were men (94%) with a mean age of 49 ± 12 years. These patients had a mean NYHA functional classification of III–IV and were previously diagnosed with significant comorbidities including hypertension and hypercholesterolemia. The clinical characteristics of patients according to aetiology of HF are summarized in *Table 1*. The ICM group showed a significant increase in age ($P < 0.01$). Significant differences were also found in left ventricular end-systolic diameter (LVESD) ($P < 0.001$), left ventricular end-diastolic diameter (LVEDD) ($P < 0.01$), and left ventricular mass index (LVMI) as well as an increase in the DCM group ($P < 0.01$) compared with CNT group. Five non-diseased donor hearts were used as CNT samples (60% male, mean age 55 ± 3 years, and EF > 50), the causes of death being cerebrovascular accident and motor vehicle accident.

Table 1 Patients characteristics according to HF aetiology

	ICM ($n = 30$)	DCM ($n = 16$)
Age (years)	54 ± 7	44 ± 13**
Gender male (%)	100	82
NYHA class	3.5 ± 0.4	3.4 ± 0.5
BMI (kg/m^2)	28 ± 4	27 ± 6
Haemoglobin (mg/dL)	14 ± 2	13 ± 2
Haematocrit (%)	41 ± 5	39 ± 6
Total cholesterol (mg/dL)	174 ± 56	127 ± 54*
Prior hypertension (%)	46	21
Prior smoking (%)	86	58*
EF (%)	24 ± 11	21 ± 8
FS (%)	17 ± 7	13 ± 8
LVESD (mm)	53 ± 9	72 ± 9***
LVEDD (mm)	63 ± 9	78 ± 9***
Left ventricle mass index (g/cm^2)	146 ± 37	210 ± 57**
Duration of disease (months)	44 ± 42	60 ± 52

Duration of disease from diagnosis of HF until heart transplant. BMI, body mass index; DCM, dilated cardiomyopathy; EF, ejection fraction; FS, fractional shortening; ICM, ischaemic cardiomyopathy; LVEDD, left ventricular end-diastolic diameter; LVESD, left ventricular end-systolic diameter; NYHA, New York Heart Association.
*$P < 0.05$.
**$P < 0.01$.
***$P < 0.001$.

3.2 Effects of HF on IMPs and EXPs levels

We analysed whether HF induced changes in the import and export of several proteins through the NPC in cardiomyocytes. Therefore, we determined the levels of IMP-β3, IMP-α2, EXP-1, and EXP-4 by western blot techniques. When we compared protein levels between HF and CNT hearts, the import and export molecules analysed were significantly increased in pathological samples (264 ± 93 vs. 100 ± 12 AU, $P = 0.001$; 163 ± 43 vs. 100 ± 30 AU, $P = 0.009$; 293 ± 130 vs. 100 ± 24 AU, $P = 0.001$; 169 ± 69 vs. 100 ± 25 AU, $P = 0.01$, respectively). Then, to compare protein levels according to aetiology of HF, ICM hearts showed higher levels of IMP-β3 (250 ± 89 vs. 100 ± 12 AU, $P < 0.0001$), IMP-α2 (169 ± 41 vs. 100 ± 30 AU, $P = 0.001$), EXP-1 (278 ± 137 vs. 100 ± 24 AU, $P < 0.0001$), and EXP-4 (181 ± 68 vs. 100 ± 25 AU, $P = 0.006$) than those in the CNT group (*Figure 1*). Furthermore, DCM hearts showed significant differences for IMP-β3 (292 ± 95 vs. 100 ± 12 AU, $P < 0.0001$), IMP-α2 (152 ± 45 vs. 100 ± 30 AU, $P = 0.025$), and EXP-1 (328 ± 109 vs. 100 ± 24 AU, $P < 0.0001$) compared with the CNT group (*Figure 1*). Levels of EXP-4 did not show statistical changes. There were not any significant differences in nuclear protein levels between the two aetiologies of HF.

Finally, we determined whether there any correlations between protein levels (IMP-α2, IMP-β3, EXP-1, and EXP-4) and clinical parameters (LVEDD, LVESD, and LVMI). The results obtained show that IMP-β3 is significantly correlated with these three clinical parameters in our group of HF patients ($r = 0.379$, $P = 0.043$; $r = 0.402$, $P = 0.034$; and $r = 0.568$, $P = 0.002$, respectively). Furthermore, the protein EXP-1 is also related with LVEDD and LVMI ($r = 0.410$, $P = 0.034$ and $r = 0.438$, $P = 0.032$, respectively). When we analysed the relationships between protein levels and clinical parameters according to HF aetiology (ischaemic or dilated group), we obtained high correlation coefficients, but they did not reach statistical significance.

3.3 Effect of HF on ran regulator protein levels

We also investigated whether HF induced changes in the regulatory proteins of the Ran system. Therefore, we determined the two forms of RanGAP1, cytoplasmatic (RanGAP1) and envelope associated form (Ran GAP1^u), and RanBP1 levels in human cardiomyocytes by western blot techniques. When we compared protein levels between HF and CNT hearts, RanGAP1 and RanGAP1^u were significantly increased in pathological hearts (162 ± 64 vs. 100 ± 33 AU, $P = 0.028$; 150 ± 63 vs. 100 ± 25 AU, $P = 0.01$, respectively), but there was no difference for RanBP1. Then, to

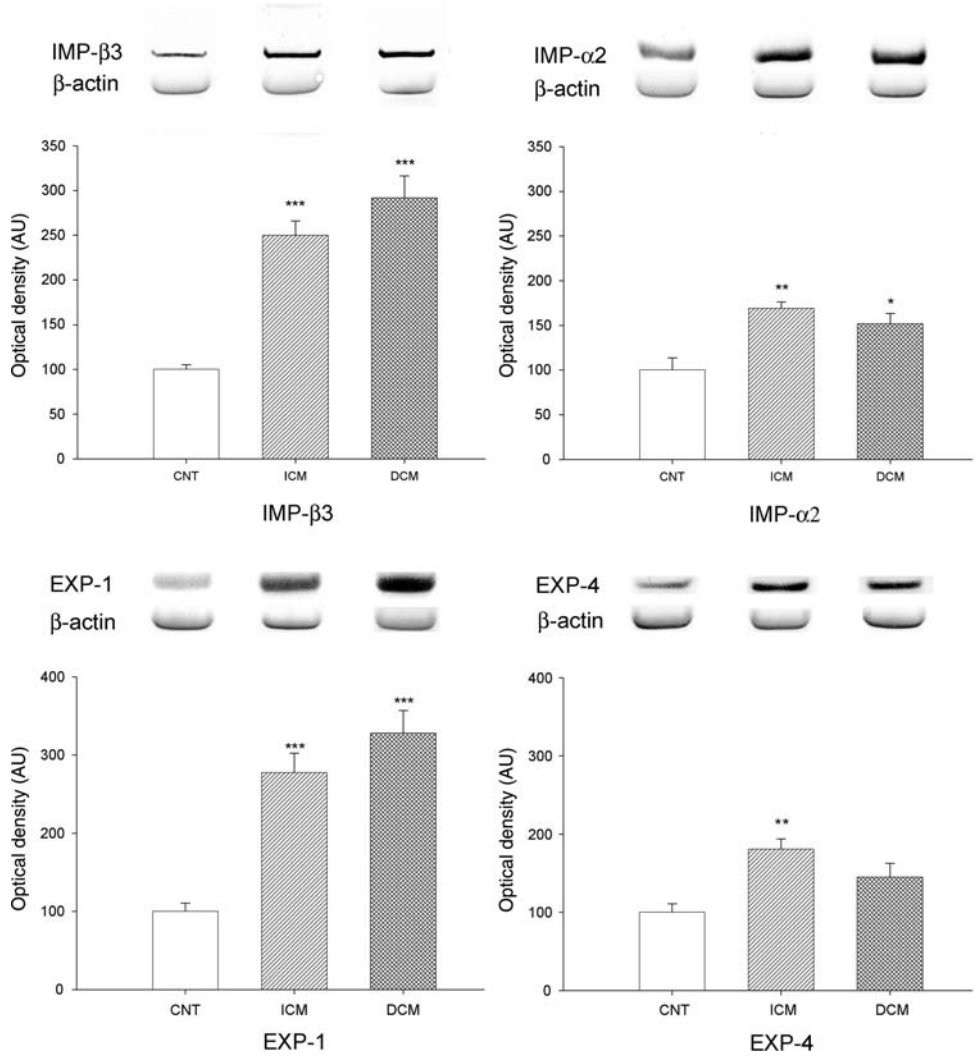

Figure 1 Influence of heart failure aetiology on the amount of some representative proteins involved in nucleocytoplasmic import (IMP-β3 and IMP-α2) and export (EXP-1 and EXP-4) analysed by western blot techniques. As shown, all proteins were significantly increased by HF. The values from the CNT group were set to 100. The data are expressed as mean ± SEM in arbitrary units (optical density) of four independent experiments. ICM, ischaemic cardiomyopathy; DCM, dilated cardiomyopathy; CNT, control. *$P < 0.05$, **$P < 0.01$, ***$P < 0.0001$ vs. CNT group.

compare the two Ran GAP1 forms according to aetiology of HF, ICM (176 ± 74 vs. 100 ± 33 AU, $P = 0.005$; 151 ± 72 vs. 100 ± 25 AU, $P = 0.012$) and DCM hearts (141 ± 39 vs. 100 ± 33 AU, $P = 0.042$ and 150 ± 48 vs. 100 ± 25 au, $P = 0.029$) had higher RanGAP1 and RanGAP1^{u} levels compared with CNT hearts (*Figure 2*). There were no significant differences for RanGAP forms between these two aetiologies, and RanBP1 levels were also not altered in HF.

3.4 Effect of HF on distribution of proteins required to nucleocytoplasmic transport

Immunofluorescence studies showed that the intensity of IMP-α2, RanGAP1, and p62 were higher in ischaemic and dilated hearts compared with CNT samples (*Figure 3*). IMP-α2 had a diffuse cytoplasmic and nuclear distribution (*Figure 3*A–C). Similar results were obtained for IMP-β3, EXP-1, and EXP-4 (data not shown). RanGAP1 showed two distribution patterns: lower surface of the nucleus and diffused on the cytoplasm (*Figure 3*D–F). Finally, Nup p62 had two nuclear distribution patterns: in the nuclear centre (*Figure 3*G) and on the low surface of the nucleus (*Figure 3*H and I). These patterns of distribution were not altered in ischaemic or dilated hearts. In all micrographs, we have observed the autofluorescence of lipofucsin particles (arrow indicated these structures). Furthermore, IMP-α2 was distributed on both the cytoplasm and nucleus, but a significant higher percentage of fluorescence was measured inside the nucleus of ischaemic (53%, $P < 0.01$) and dilated hearts (96%, $P < 0.01$) than outside (*Figure 4*). Similar distribution was observed for IMP-β3 (data not shown).

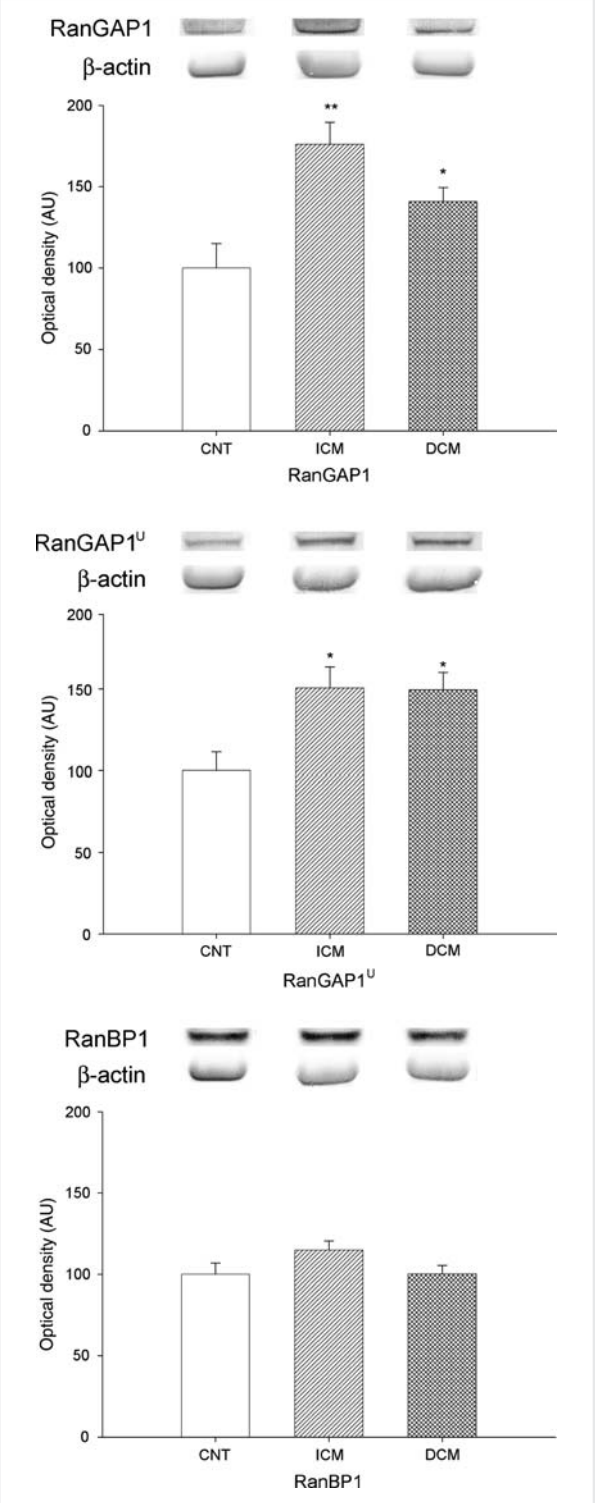

Figure 2 Effect of HF on Ran regulator protein levels (RanGAP1, RanGAP1^{u}, and RanBP1). As shown, RanGAP1 and RanGAP1^{u} were significantly affected by HF, but not RanBP1. The values from the CNT group were set to 100. The data are expressed as mean ± SEM in arbitrary units (optical density) of four independent experiments. ICM, ischaemic cardiomyopathy; DCM, dilated cardiomyopathy; CNT, control. *$P < 0.05$, **$P < 0.01$ vs. CNT group.

Then, when we analysed the relative fluorescence between cytoplasm (RanGAP1 diffuse cytoplasmic pattern) and nucleus (RanGAP1^{u} associated to NPCs), no significant differences were obtained either in ischaemic or dilated hearts. The Ran forms appeared distributed in a similar amount in the nucleus and cytoplasm in dilated hearts, and nuclear fluorescence was slightly decreased in ischaemic hearts (7%) (*Figure 4*). There were not differences for RanBP1 distribution in the different samples.

3.5 Effect of HF on expression of p62 and NPC morphology

In addition to the analysis of the proteins involved in the nucleocytoplasmic transport, we also studied the effects of HF on the amount of protein associated with NPC, such as Nup p62. Immunoblot analysis showed that amount of p62 was significantly increased in pathological hearts compared with CNT samples (193 ± 88 vs. 100 ± 5, $P = 0.019$). According to aetiology of HF, Nup p62 was also increased in hearts with ICM (180 ± 66 vs. 100 ± 5, $P < 0.001$) and DCM (209 ± 108 vs. 100 ± 5, $P = 0.024$) (*Figure 5*). No statistical differences were found between these two aetiologies.

Ultrastructure analysis captured NPCs spanning the nuclear envelope in specialized domains formed by fusion of the inner and outer nuclear membrane (*Figure 6*). In the nuclear envelope of human cardiomyocytes pathological hearts had 0.39 ± 0.03 NPCs/μm similar than CNT hearts (*Table 2*). This fact was comparable according to HF aetiology, ischaemic (0.40 ± 0.04 NPCs/μm) and dilated samples (0.36 ± 0.07 NPCs/μm) (*Table 2*).

Furthermore, the NPC from ischaemic cardiomyocytes had an overall diameter of 85.2 ± 4.1 nm, a significantly lower value than the diameter of NPCs from CNT ($P = 0.005$) or dilated hearts ($P = 0.04$). Pathological hearts showed a significant inverse correlation between the number of NPCs and the overall diameters of cardiomyocytes, either in ischaemic or dilated samples (*Table 2*). Finally, analysing the structure of NPCs at nanoscale resolution identified that the central channel was occupied by dense material in several nuclear pores (white arrows in *Figure 6C* and *D*). In ischaemic cardiomyocytes, $32.1 \pm 2.9\%$ of nuclear pores adopt this configuration ($P = 0.026$), in dilated samples was $24.8 \pm 3.3\%$, and only $22.1 \pm 2.4\%$ in CNT hearts. Thus, in ischaemic cardiomyocytes, NPCs had low diameter and high percentage with the dense material in the central channel (*Table 2*).

4. Discussion

The present study offers several insights into the nucleocytoplasmic transport in human hearts of patients with HF. First, we determined the quantity of nuclear transport proteins by western blot techniques in cardiac tissue, and the results showed that amount of import and export factors are significantly increased in patients with DCM and ICM compared with the CNT group. Second, the Ran regulator system showed higher levels of RanGAP1 and RanGAP1^{u} in HF hearts. Third, immunofluorescence images showed that distribution patterns of these proteins were not altered by HF aetiology, and there was higher flourescence intensity in pathological hearts than CNT samples. Fourth, we found

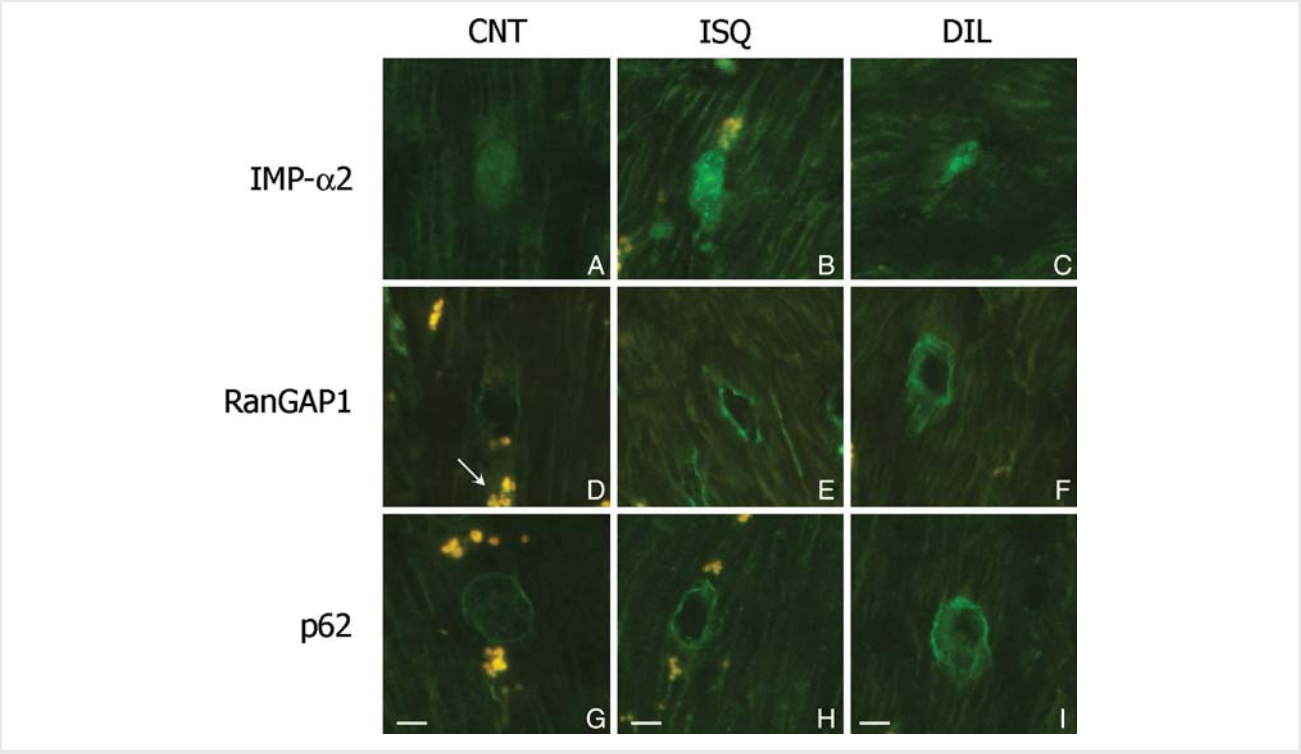

Figure 3 Effect of HF on cell distribution of some proteins involved in nucleocytoplasmic transport in human cardiomyocytes of left ventricle. Immunofluoresence for importin-α2 (IMP-α2) (*A–C*), RanGAP1 and RanGAP1^{u} (*D–F*) and p62 (*G–I*) according to HF aetiology, ischaemic (ICM) and dilated (DCM) cardiomyopathy compared with control group (CNT). Arrow indicates the fluorescence of lipofucsin particles. All the micrographs correspond to four independent experiments. The bar represents 10 μm.

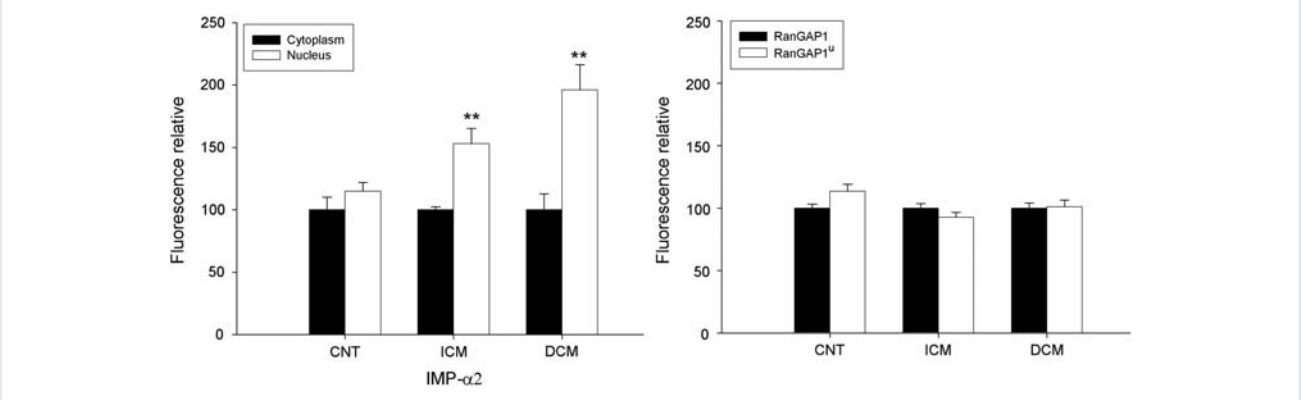

Figure 4 Bar graph comparing the fluorescence intensity in cytoplasm and into nucleus of importin-α2 (IMP-α2), and the fluorescence of the two forms of Ran regulators (RanGAP1 in the cytoplasm and RanGAP1^{u} in the nuclear membrane). The values from the cytoplasm were set to 100. The data are expressed as mean ± SEM of four experiments. ICM, ischaemic cardiomyopathy; DCM, dilated cardiomyopathy; CNT, control. $^{**}P < 0.01$.

that density of the NPCs was comparable in HF hearts (ischaemic or dilated) with CNTs despite the significant increase in the amounts of IMPs, EXPs, and Nup p62.

Several authors have demonstrated that nucleocytoplasmic trafficking machinery associated with nuclear translocation of cardiac transcription factors underscore its plasticity according to cell requirements. The group of Lidsky *et al.*[6] has shown that cells infected with different cardioviruses result in similar alterations of the nucleocytoplasmic traffic, but by different mechanisms. Perez-Terzic *et al.*[7] also describe direct inhibition of nuclear import and increased export in cellular hypertrophy in cardiomyocyte cultures.

To explain the effect of HF on the import to the nucleus, we first analysed whether this syndrome affects the amount of

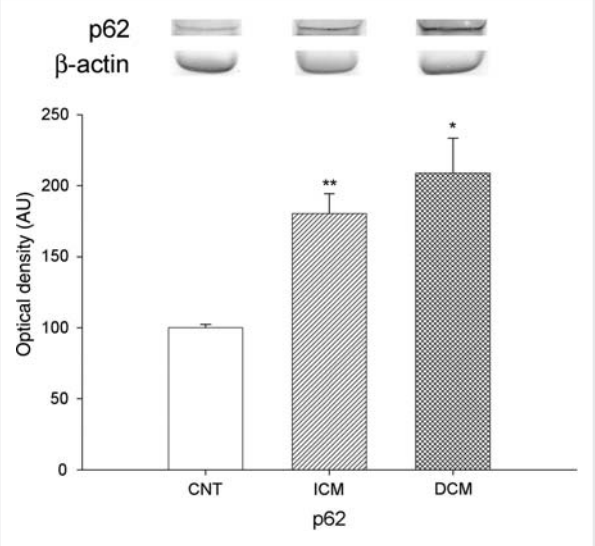

Figure 5 Effect of HF on Nup p62 protein levels. As shown, Nup p62 was significantly increased in HF. The values from the CNT group were set to 100. The data are expressed as mean ± SEM in arbitrary units (optical density) of four independent experiments. ICM, ischaemic cardiomyopathy; DCM, dilated cardiomyopathy; CNT, control. $^{**}P < 0.001$, $^{*}P < 0.05$ vs. CNT group.

IMP-α2 and IMP-β3, representative factors involved in nuclear import, using western blot techniques. We found that human hearts with ischaemic or DCM showed a significant increase in the quantity of these proteins that had an important role in the relaying information between the cytoplasm and the nucleus (import of histones and ribosomal proteins).[20]

Moreover, HF could also affect the nuclear export of proteins. Nucleocytoplasmic transport is a continuous process so transporting factors should return to their initial sites for following rounds of transport,[20] the protein EXP-1 is involved in the nuclear export of these shuttling proteins.[21] Thus, the increase in the IMP-α2 and IMP-β3 proteins are associated with a high amount of EXP-1. In addition, alterations in the amount of this factor could result in quantitative changes in the nuclear export of those cargoes and in the regulation of several pathological processes that depend on this protein.[22] Therefore, we analysed the amount of EXP-1 in ischaemic and DCM human hearts and found an increase in the amount of this EXP. However, only ischaemic hearts showed a significant increase in EXP-4 protein that has been shown to mediate the nuclear export of several factors that regulate cell proliferation, differentiation, and apoptosis (eIF-5A and Smad3).[23,24] This fact could indicate that these processes, included in the left ventricular (LV) structural remodelling, were less in hearts with dilated than ICM. However, analysis of the nucleus in our human cardiomyocytes from HF patients by transmission electron microscopy did not show perturbation of the nuclear envelope, clustering of nuclear pores and chromatin condensation, as specific nuclear apoptotic figures.[25,26]

On the other hand, Ran-related factors amplifies the GTPase activity of Ran, which plays the key role in the formation of diverse transporting complexes, and this amplification is higher in the presence of RanBP1.[27,28] RanGAP1^{u} is localized to fibrils of the NPC cytoplasmic surface, regulating the formation and the transference through the NPC of the import protein complex. Then, the dissociation of exported transport complexes due to GTP hydrolysis is stimulated by RanGAP1, which is found only in the cytoplasm, or RanGAP1^{u}[20]. Our results showed that the amount of RanGAP1 and RanGAP1^{u} were also increased in HF hearts irrespective of aetiology, but RanBP1 (protein-activating RanGAP1) was not altered by this syndrome.

Then, when we analysed the intracellular distribution of nucleocytoplasmic machinery by immunofluorescence, we did not find alterations in the distribution patterns in hearts with ischaemic or DCM compared with CNT samples. Although, pathological cardiomyocytes had higher fluorescence intensity and the percentage of IMPs inside nucleus is higher than outside. This finding could show that there is an increase in the nuclear import of different cargoes in HF. Furthermore, not significant differences were obtained for Ran-related factors between nucleus (RanGAP1^{u}) or cytoplasm (RanGAP1^{u} or RanGAP1) distribution. These data suggest that both nuclear import and export are increased, and there is a balance between these two cell compartments.

LV remodelling plays a critical role in the development of chronic HF and involves LV hypertrophy and dilatation. These processes are associated with loss of cardiac myocytes (by necrosis or apoptosis) that result in sites of replacement of fibrosis, a restructuring of cytoskeleton and mitochondrial alterations.[29,30] As a consequence *de novo* protein synthesis that depends on the import to nucleus of translation factors and the export of RNAs species from the nucleus of cardiomyocytes is required. This fact is in accordance with our results, an increase in the nucleocytoplasmic trafficking machinery. Furthermore, as this adaptative process (LV remodelling) occurs either in ischaemic or DCM, we did not find significant differences in the amount of IMPs, EXPs, or Ran-related factors between these two aetiologies.

Finally, NPCs play an important role in the transport between the nucleus and the cytoplasm.[31] As previously commented, cardiomyocytes of patients diagnosed with HF undergo phenotypic changes requiring the increased processing and delivery of genetic information across the nuclear envelope. Translocation occurs through NPC, which span the nuclear envelope and gate bidirectional nucleocytoplasmic exchange. Moreover, in response to changes in the functional and metabolic state of the cell, nuclear pores adopt distinct conformations indicating that traffic through them is a dynamic process.[8,32,33]

Using electron microscopy, we found that density of the NPCs was comparable in HF hearts (ischaemic or dilated) with CNTs despite significant increase in the amount of IMPs, EXPs, and Nup p62. Moreover, analysing the structure of nuclear pores identified that several complexes had the central channel occupied by dense material which has been proposed to represent a central transporter. This specialized structure could increase the gating and translocation of molecules through nuclear pore.[8,33] Thus, ischaemic cardiomyocytes were characterized by a low overall diameter and a high percentage of NPCs with dense material. This fact could represent a structural basis for selective transport through the nuclear envelope and the structure plasticity of the

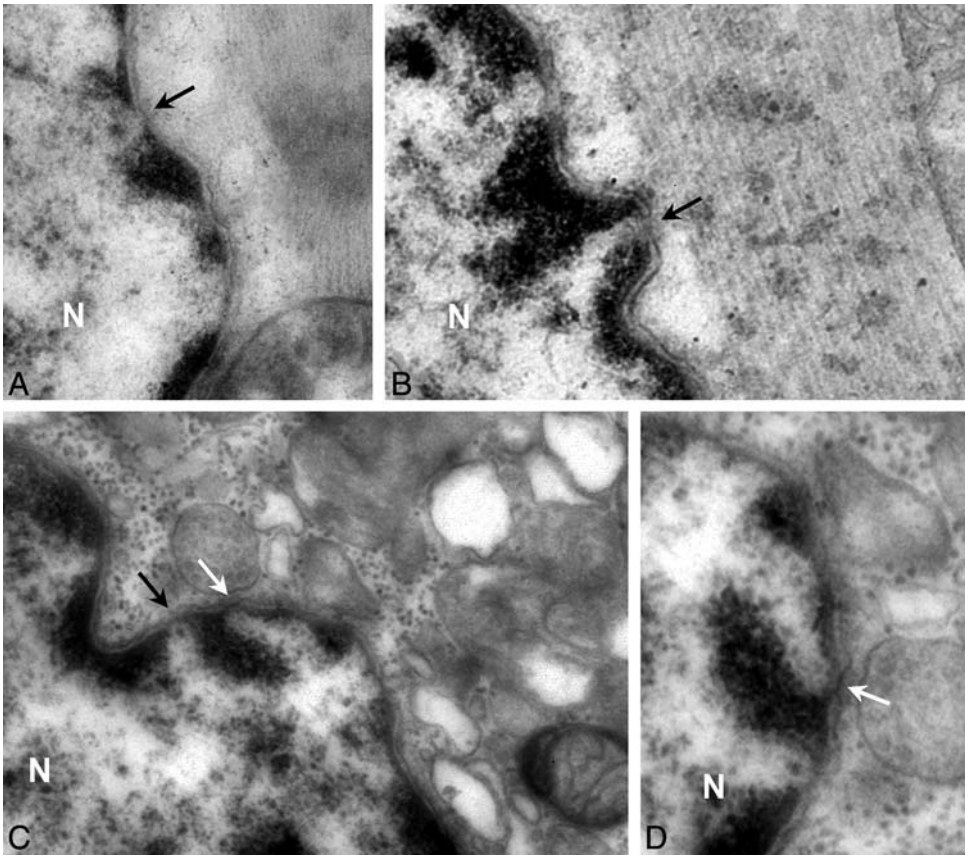

Figure 6 NPC in nuclear envelope of human cardiomyocytes by transmission electron microscopy. Cross sections of a single nucleus in CNT (*A*), dilated (*B*), or ischaemic (*C* and *D*) samples. Arrows indicate the nuclear pores with a distinct configuration: without (black arrow) or with (white arrow) dense material in the central channel. Transmission electron microscopy micrographs did not show apoptotic figures (chromatin condensation, perturbation of nuclear envelope and clustering of nuclear pores). N indicate nucleus. Bar represent: 200 nm.

Table 2 Characteristics of cardiac NPCs according to HF aetiology

	NPCs (μm)	NPCs diameter (nm)	NPCs number vs. NPCs diameter	% NPC with dense material
Control	0.40 ± 0.06	108.7 ± 6.9	$r = 0.20$	22.1 ± 2.4
Pathological	0.39 ± 0.03	90.2 ± 4.1*	$r = -0.43$*	30.0 ± 2.3*
Ischaemic cardiomyopathy	0.40 ± 0.04	85.2 ± 4.1**	$r = -0.36$	32.1 ± 2.9*
Dilated cardiomyopathy	0.36 ± 0.07	101.9 ± 9.3	$r = -0.57$	24.8 ± 3.3

Measurements are expressed as mean ± SE. A total of 10–12 sections was used in the determination of NPC values. The number of NPCs analysed was 80 under each pathological condition.
Significant difference from control values: *$P < 0.05$; **$P < 0.01$.
Significance of correlation coefficient (r):*$P < 0.05$.

cardiac NPC in response to specific cellular conditions (pathological remodelling), providing a mechanism for distinct regulation of nuclear transport through the nuclear envelope.

Although the present study has shown that HF increases the amount and nuclear distribution of the representative proteins involved in nucleocytoplasmic transport in human LV cardiomyocytes, further studies are necessary to analyse other factors involved in transport through the NPC, to determine the efficiency of nucleocytoplasmic transport in ischaemic and dilated human hearts. One limitation of this study is the intrinsic variability of the samples, given they originate from human hearts, whose conditions (treatment they undergo) are not as standardized as those of studies using cell cultures. Furthermore, it would be interesting to analyse the effect of HF on direct nucleocytoplasmic transport (synthesis of proteins and transport of labelled molecules).

In summary, the present study establishes for the first time that HF influences on nucleocytoplasmic trafficking machinery in human hearts irrespective of ischaemic or dilated aetiology. Our results demonstrate an important increase in the quantity of IMPs, EXPs, and Ran-related factors in patients undergoing heart transplant. Moreover, NPCs suffered an adaptative process, acquiring a different configuration and morphology under increased demand for nucleocytoplasmic transport, such as during pathological remodelling in ICM. In this regard, identifying the mechanism that modulates the structure of the cardiac NPC would provide important information about regulators of nuclear transport in HF.

Acknowledgements

The authors thank the Transplant Coordination Unit (Hospital Universitario La Fe, Valencia, Spain) for their help in obtaining the samples, and Professor Dr Jaime Renau Piqueras and Dra Pilar Marín (Cell Biology and Pathology Section of Research Center, Hospital Universitario La Fe, Valencia, Spain) for their collaboration in technical approach of this paper. Furthermore, we are grateful to Inmaculada Montserrat and Lorena Gomez (technicians at the Research Center, Hospital Universitario La Fe, Valencia, Spain) for her assistance in optical and electron microscopy procedures.

Conflict of interest: none declared.

Funding

This work was supported by grants from the NIH 'Fondo de Investigaciones Sanitarias del Instituto de Salud Carlos III', [REDINSCOR 06/0003/1001, Project PI07/0462].

References

1. Rosca MG, Vazquez EJ, Kerner J, Parland W, Chandler MP, Stanley W *et al.* Cardiac mitochondria in heart failure: decrease in respirasomes and oxidative phosphorylation. *Cardiovasc Res* 2008;**80**:30–39.
2. Hein S, Kostin S, Heling A, Maeno Y, Schaper J. The role of the cytoskeleton in heart failure. *Cardiovasc Res* 2000;**45**:273–278.
3. Monreal G, Nicholson LM, Han B, Joshi MS, Phillips AB, Wold LE *et al.* Cytoskeletal remodelling of desmin is a more accurate measure of cardiac dysfunction than fibrosis or myocytes hypertrophy. *Life Sci* 2008;**83**:786–794.
4. Cieniewski-Bernard C, Mulder P, Henry JP, Drobecq H, Dubois E, Pottiez G *et al.* Proteomic analysis of left ventricular remodelling in an experimental model of heart failure. *J Proteome Res* 2008;**7**:5004–5016.
5. Yoneda Y. Nucleocytoplasmic protein traffic and its significance to cell function. *Genes Cells* 2001;**5**:777–787.
6. Lidsky PV, Hato S, Bardina MV, Aminev AG, Palmenberg AC, Sheval EV *et al.* Nucleocytoplasmic traffic disorder induced by cardioviruses. *J Virol* 2006;**80**:2705–2717.
7. Perez-Terzic C, Gacy AM, Bortolon R, Dzeja PP, Puceat M, Jaconi M *et al.* Directed inhibition of nuclear import in cellular hypertrophy. *J Biol Chem* 2001;**276**:20566–20571.
8. Perez-Terzic C, Gacy AM, Bortolon R, Dzeja PP, Puceat M, Jaconi M *et al.* Structural plasticity of the cardiac nuclear pore complex in response to regulators of nuclear import. *Circ Res* 1999;**84**:1292–1301.
9. Görlich D, Kutay U. Transport between the cell nucleus and the cytoplasm. *Annu Rev Cell Dev Biol* 1999;**15**:607–660.
10. Cook A, Bono F, Jinek M, Conti E. Structural biology of nucleocytoplasmic transport. *Annu Rev Biochem* 2007;**76**:647–671.
11. Paschal BM, Gerace L. Identification of NTF2, a cytosolic factor for nuclear import that interacts with nuclear pore complex protein p62. *J Cell Biol* 1995;**129**:925–937.
12. Stewart M. Molecular mechanism of the nuclear import cycle. *Nat Rev Mol Cell Biol* 2007;**8**:195–208.
13. Fukuda M, Asano S, Nakamura T, Adachi M, Yoshida M, Yanagida M *et al.* CRM1 is responsible for intracellular transport mediated by the nuclear export signal. *Nature* 1997;**390**:308–311.
14. Richards SA, Carey KL, Macara IG. Requirement of guanosine triphosphate-bound Ran for signal-mediated nuclear protein export. *Science* 1997;**276**:1842–1844.
15. Swedberg K, Cleland J, Dargie H, Drexler H, Follath F, Komajda M *et al.* Guidelines for the diagnosis and treatment of chronic heart failure: executive summary (update 2005): the Task Force for the Diagnosis and Treatment of Chronic Heart Failure of the European Society of Cardiology. *Eur Heart J* 2005;**26**:1115–1140.
16. Lowry OH, Rosenbrough NJ, Farr AR, Randall RJ. Protein measurement with the Folin phenol reagent. *J Biol Chem* 1951;**193**:265–275.
17. Azorín I, Portolés M, Marín P, Lázaro-Diéguez F, Megías L, Egea G *et al.* Prenatal ethanol exposure alters the cytoskeleton and induces glycoprotein microheterogeneity in rat newborn hepatocytes. *Alcohol Alcohol* 2004;**39**:203–212.
18. Reynolds ES. The use of lead citrate at high pH as an electron-opaque stain in electron microscopy. *J Cell Biol* 1963;**17**:208–212.
19. Marín MP, Tomas M, Esteban-Pretel G, Megías L, López-Iglesias C, Egea G *et al.* Chronic etanol exposure induces alterations in the nucleocytoplasmic transport in growing astrocytes. *J Neurochem* 2008;**106**:1914–1928.
20. Sorokin AV, Kim ER, Ovchinnikov LP. Nucleocytoplasmic transport of proteins. *Biochemistry (Mosc)* 2007;**72**:1439–1457.
21. Johnson AW, Lund E, Dahlberg J. Nuclear export of ribosomal subunits. *Trends Biochem Sci* 2002;**27**:580–585.
22. Harrison BC, Roberts CR, Hood DB, Sweeney M, Gould JM, Bush EW *et al.* The CRM1 nuclear export receptor controls pathological cardiac gene expression. *Mol Cell Biol* 2004;**24**:10636–10649.
23. Li AL, Li HY, Jin BF, Ye QN, Zhou T, Yu XD *et al.* A novel eIF5A complex functions as a regulator of p53 and p53-dependent apoptosis. *J Biol Chem* 2004;**279**:49251–49258.
24. Kurisaki A, Kurisaki K, Kowanetz M, Sugino H, Yoneda Y, Heldin CH *et al.* The mechanism of nuclear export of Smad3 involves exportin 4 and Ran. *Mol Cell Biol* 2006;**26**:1318–1832.
25. Yasuhara S, Zhu Y, Matsui T, Tipirneni N, Yasuhara Y, Kaneki M *et al.* Comparison of comet assay, electrón microscopy, and flow cytometry for detection of apoptosis. *J Histochem Cytochem* 2003;**51**:873–885.
26. Kihimark M, Imreh G, Hallberg E. Sequential degradation of proteins from the nuclear envelope during apoptosis. *J Cell Sci* 2001;**114**:3643–3653.
27. Floer M, Blobel G, Rexach M. Disassembly of RanGTP-karyopherin beta complex, an intermediate in nuclear protein import. *J Biol Chem* 1997;**272**:19538–19546.
28. Lounsbury KM, Macara IG. Ran-binding protein 1 (RanBP1) forms a ternary complex with Ran and karyopherin beta and reduces Ran GTPase-activating protein (RanGAP) inhibition by karyopherin beta. *J Biol Chem* 1997;**272**:551–555.
29. Pomar F, Cosin J, Portoles M, Faura M, Renau-Piqueras J, Hernandiz A *et al.* Functional and ultrastructural alterations of canine myocardium subjected to very brief coronary occlusions. *Eur Heart J* 1995;**16**:1482–1490.
30. Timonen P, Magga J, Risteli J, Punnonen K, Vanninen E, Turpeinen A *et al.* Cytokines, interstitial collagen and ventricular remodelling in dilated cardiomyopathy. *Int J Cardiol* 2008;**124**:293–300.
31. Stoffler D, Feja B, Fahrenkrog B, Walz J, Typke D, Aebi U. Cryo-electron tomography provides novel insights into nuclear pore architecture: implications for nucleocytoplasmic transport. *J Mol Biol* 2003;**328**:119–130.
32. Antonin W, Ellenberg J, Dultz E. Nuclear pore complex assembly through the cell cycle: regulation and membrane organization. *FEBS Lett* 2008;**582**:2004–2016.
33. Perez-Terzic C, Behfar A, Méry A, van Deursen JM, Terzic A, Pucéat M. Structural adaptation of the nuclear pore complex in stem cell-derived cardiomyocytes. *Circ Res* 2003;**92**:444–452.